

## A similarity hypothesis for the two-point correlation tensor in a temporally evolving plane wake

By D. W. Ewing<sup>1</sup>, W. K. George<sup>2</sup>, R. D. Moser<sup>3</sup>, AND M. M. Rogers<sup>4</sup>

### 1. Motivation and objectives

It has long been known that the equations that govern the evolution of the single-point moments, such as the mean velocity or the turbulent Reynolds stresses, admit similarity solutions for many of the basic shear flows (*e.g.* George 1989 or Tennekes and Lumley 1972). In this approach, it is argued that the flow evolves such that all of the terms in the governing equations make the the same relative contribution so the flow reaches an 'equilibrium' or similarity state. In many cases the initial conditions of the flow are inconsistent with the hypothesized similarity solutions so these solutions are, at most, an approximation of the flows asymptotic state. However, the agreement between the predictions of the theory and experimental data (*e.g.*, Wygnanski *et al.* 1989) suggests that flows do approach such an asymptotic state.

Traditionally (*e.g.*, Tennekes and Lumley 1972), it was argued that this asymptotic state is universal for all flows of a particular type (*e.g.*, all plane wakes). However, this argument is not consistent with the measurements in the far field of plane wakes reported by Wygnanski *et al.* (1989), who found that the similarity profiles of the normal Reynolds stresses (particularly the streamwise component) differed for different types of wake generators. George (1989) argued that this occurred because the governing equation for the similarity profile of the turbulent kinetic energy contained a constant that depended on the growth rate of the flow. Consequently, George (1989) concluded that the similarity profiles for the normal stresses would not be universal unless the growth rates of all wakes were the same, which was not the case for the wakes studied by Wygnanski *et al.* (1986). (A similar conclusion was reached from a later analysis of the governing equations for the individual normal stresses; *e.g.*, George 1994 or Ewing and George 1994.) George (1989) attributed the differences in the growth rates of the wakes (and hence the asymptotic states) to differences in the coherent structures produced by the bodies generating the wake.

1 Department of Mechanical Engineering, Queen's University, Kingston, Canada, K7L 3N6.

2 Department of Mechanical and Aerospace Engineering, State University of New York at Buffalo, Amherst, NY, 14260.

3 Department of Theoretical and Applied Mechanics, University of Illinois at Urbana-Champaign, Urbana, IL 61801.

4 NASA Ames Research Center.

It is now widely recognized that coherent structures play an integral role in many of the processes that determine the growth rate of a turbulent flow, including the entrainment of irrotational flow and the gross mixing of the fluid across the layer. A question that has not yet been resolved is whether the structures in the flow themselves (or more properly the coherent structures and the probability density functions describing their occurrences) approach an 'equilibrium' or similarity state when the single-point moments measured in the flow agree with the predictions of the similarity hypothesis. That is, can all of the statistical measures of the structures (the single-point moments being the simplest) at different points in a flow's evolution be related by a similarity transformation.

The primary objective of this research is to examine whether the governing equations for more complex statistical measures of the structures in the temporally evolving plane wake admit similarity solutions. (In the initial stage of this research it was established that the governing equations for the mean momentum and the Reynolds stresses admit similarity solutions, *v. Moser et al. 1995*). The two-point velocity correlation tensor was chosen because it contains more information about the turbulent structure than the single-point moments and it is often used in attempts to educe coherent structures from the flow (*e.g.*, Grant 1958 or Payne and Lumley 1967). There have been few previous attempts to demonstrate that the governing equations for these two-point correlations admit similarity solutions in non-homogeneous flows. Ewing and George (1994) and Ewing (1995) demonstrated that the governing equations for the two-point velocity correlation tensor in the far fields of the spatially evolving axisymmetric and plane jets admit similarity solutions. However, in both of these cases the predictions of the similarity hypotheses were not tested using experimental data, so it was not determined if these similarity solutions are accurate descriptions of real shear flows. This question is addressed in this research using data from Direct Numerical Simulations of the temporally evolving wake computed by Moser and Rogers (1994).

## 2. Accomplishments

### 2.1 Theoretical analysis

In the temporally evolving wake, shown in Fig. 1, a momentum deficit spreads in one non-homogeneous direction,  $x_2$ , as the flow evolves in time. The other two directions, including the direction of the mean flow,  $x_1$ , are homogeneous. Consequently, the governing equations for the two-point velocity correlations in this flow can be written as

$$\begin{aligned} & \frac{\partial \overline{u_i u'_j}}{\partial t} + (U_1 - U'_1) \frac{\partial \overline{u_i u'_j}}{\partial \zeta} = \\ & -\frac{1}{\rho} \left[ \frac{\partial}{\partial \zeta} \left( \overline{p u'_j} \delta_{i1} - \overline{p' u_i} \delta_{j1} \right) + \frac{\partial \overline{p u'_j}}{\partial x_2} \delta_{i2} + \frac{\partial \overline{p' u_i}}{\partial x'_2} \delta_{j2} + \frac{\partial}{\partial \gamma} \left( \overline{p u'_j} \delta_{i3} - \overline{p' u_i} \delta_{j3} \right) \right] \\ & - \frac{\partial}{\partial \zeta} \left( \overline{u_1 u_i u'_j} - \overline{u'_1 u_i u'_j} \right) - \frac{\partial \overline{u_2 u_i u'_j}}{\partial x_2} - \frac{\partial \overline{u'_2 u_i u'_j}}{\partial x'_2} - \frac{\partial}{\partial \gamma} \left( \overline{u_3 u_i u'_j} - \overline{u'_3 u_i u'_j} \right) \end{aligned}$$

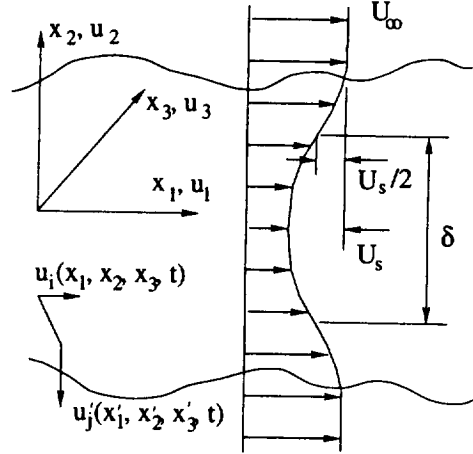


FIGURE 1. Geometry of the temporally evolving wake

$$-\overline{u'_j u_2} \frac{\partial U_1}{\partial x_2} \delta_{i1} - \overline{u_i u'_2} \frac{\partial U_1}{\partial x'_2} \delta_{j1} + \nu \left( 2 \frac{\partial^2}{\partial \zeta^2} + \frac{\partial^2}{\partial x_2^2} + \frac{\partial^2}{\partial x_2'^2} + 2 \frac{\partial^2}{\partial \gamma^2} \right) \overline{u_i u'_j}, \quad (1)$$

where  $\zeta = x_1 - x'_1$ ,  $\gamma = x_3 - x'_3$ ,  $U_1$  is the mean velocity in the  $x_1$ -direction, and  $u_i$  are the fluctuating velocity components in the  $x_i$  directions. In these equations, the primed variables are evaluated at one arbitrary point in space while the unprimed variables are evaluated at a second arbitrary point. The two-point velocity correlations must also satisfy initial conditions and a number of boundary conditions; i.e.,

$$\lim_{x_2, x_2', \zeta, \gamma \rightarrow \pm\infty} \overline{u_i u'_j} = 0, \quad (2)$$

assuming the turbulence in the free stream is negligible.

Following the approach outlined by George (1989), it is hypothesized that the governing equations for the two-point correlation tensor admit similarity solutions given by

$$\overline{u_i(x_1, x_2, x_3, t) u'_j(x'_1, x'_2, x'_3, t)} = Q^{i,j}(t) q_{i,j}(\xi, \eta, \eta', \zeta, *), \quad (3a)$$

$$\overline{p(x_1, x_2, x_3, t) u'_j(x'_1, x'_2, x'_3, t)} = P_1^{j,i}(t) p_{j,i}^1(\xi, \eta, \eta', \zeta, *), \quad (3b)$$

$$\overline{p'(x'_1, x'_2, x'_3, t) u_i(x_1, x_2, x_3, t)} = P_2^{i,j}(t) p_{i,j}^2(\xi, \eta, \eta', \zeta, *), \quad (3c)$$

$$\overline{u_k u_i u'_j} = T_1^{k,i,j}(t) t t_{k,i,j}^1(\xi, \eta, \eta', \zeta, *), \quad (3d)$$

$$\overline{u_i u'_k u'_j} = T_2^{i,k,j}(t) t t_{i,k,j}^2(\xi, \eta, \eta', \zeta, *), \quad (3e)$$

where

$$\xi = \frac{\zeta}{\delta_1(t)} = \frac{x_1 - x'_1}{\delta_1(t)}, \quad \eta = \frac{x_2}{\delta(t)}, \quad \eta' = \frac{x'_2}{\delta(t)}, \quad \zeta = \frac{\gamma}{\delta_3(t)} = \frac{x_3 - x'_3}{\delta_3(t)}, \quad (3f)$$

and the \* in Eqs. 3a -3e indicate that the solutions may depend on the source conditions of the flow. At this point the length scales  $\delta_1$  and  $\delta_3$  are arbitrary.

The allowable choices for these scales are determined by examining the equations of motion. The length scale used to scale the  $x_2$  is equal to the scale used in the single-point analysis,  $\delta(t) \propto (t - t_o)^{1/2}$  (Moser *et al.* 1995), since the similarity solutions for the single- and two-point correlations must be consistent in the limit when the separation distance between the two points is zero. Here,  $t_o$  is the location of the virtual origin of the wake.

Substituting these hypothesized solutions for the two point correlations and the similarity solution for the mean velocity given by (Moser *et al.* 1995)

$$U_{1\infty} - U_1(x_2, t) = U_s(t)f(\eta) \quad (4)$$

into Eq. 1 yields

$$\begin{aligned} & \left[ \frac{dQ^{i,j}}{dt} \right] q_{i,j} - \left[ \frac{Q^{i,j}}{\delta_1} \frac{d\delta_1}{dt} \right] \xi \frac{\partial q_{i,j}}{\partial \xi} - \left[ \frac{Q^{i,j}}{\delta} \frac{d\delta}{dt} \right] \left( \eta \frac{\partial}{\partial \eta} + \eta' \frac{\partial}{\partial \eta'} \right) q_{i,j} - \left[ \frac{Q^{i,j}}{\delta_3} \frac{d\delta_3}{dt} \right] \zeta \frac{\partial q_{i,j}}{\partial \zeta} \\ & + \left[ \frac{U_s(t)Q^{i,j}}{\delta_1} \right] \{f(\eta') - f(\eta)\} \frac{\partial q_{i,j}}{\partial \xi} = -\frac{1}{\rho} \left( \left[ \frac{P_1^{j,j}}{\delta_1} \right] \frac{\partial p_{i,j}^1}{\partial \xi} \delta_{i1} - \left[ \frac{P_2^{i,j}}{\delta_1} \right] \frac{\partial p_{i,j}^2}{\partial \xi} \delta_{j1} \right. \\ & + \left[ \frac{P_1^{j,j}}{\delta} \right] \frac{\partial p_{i,j}^1}{\partial \eta} \delta_{i2} + \left[ \frac{P_2^{i,j}}{\delta} \right] \frac{\partial p_{i,j}^2}{\partial \eta'} \delta_{j2} + \left[ \frac{P_1^{j,j}}{\delta_3} \right] \frac{\partial p_{i,j}^1}{\partial \zeta} \delta_{i3} - \left[ \frac{P_2^{i,j}}{\delta_3} \right] \frac{\partial p_{i,j}^2}{\partial \zeta} \delta_{j3} \left. \right) \\ & - \left[ \frac{T_1^{1,i,j}}{\delta_1} \right] \frac{\partial tt_{1,i,j}^1}{\partial \xi} + \left[ \frac{T_2^{i,1,j}}{\delta_1} \right] \frac{\partial tt_{i,1,j}^2}{\partial \xi} - \left[ \frac{T_1^{2i,j}}{\delta} \right] \frac{\partial tt_{2i,j}^1}{\partial \eta} - \left[ \frac{T_2^{i,2j}}{\delta} \right] \frac{\partial tt_{i,2j}^2}{\partial \eta'} \\ & - \left[ \frac{T_1^{3i,j}}{\delta_3} \right] \frac{\partial tt_{3i,j}^1}{\partial \zeta} + \left[ \frac{T_2^{i,3j}}{\delta_3} \right] \frac{\partial tt_{i,3j}^2}{\partial \zeta} + \left[ \frac{Q^{2,j}U_s}{\delta} \right] q_{2,j} \frac{df}{d\tilde{\eta}} \Big|_{\tilde{\eta}=\eta} \delta_{i1} + \left[ \frac{Q^{i,2}U_s}{\delta} \right] q_{i,2} \frac{df}{d\tilde{\eta}} \Big|_{\tilde{\eta}=\eta'} \delta_{j1} \\ & + \nu \left( 2 \left[ \frac{Q^{i,j}}{\delta_1^2} \right] \frac{\partial^2}{\partial \xi^2} + \left[ \frac{Q^{i,j}}{\delta^2} \right] \frac{\partial^2}{\partial \eta^2} + \left[ \frac{Q^{i,j}}{\delta^2} \right] \frac{\partial^2}{\partial \eta'^2} + 2 \left[ \frac{Q^{i,j}}{\delta_3^2} \right] \frac{\partial^2}{\partial \zeta^2} \right) q_{i,j}, \quad (5) \end{aligned}$$

where the time-dependent portion of each term is contained in square brackets. It is possible to remove the time dependence from these equations if the time-dependent portion of the all terms in each equation are proportional, leaving a set of equations for the similarity solutions in terms of the similarity variables and the constants whose values depend on the ratios of the time-dependent terms. In this case, the similarity solutions again represent an 'equilibrium' solution for the governing equations since all of the terms make the same relative contribution as the flow evolves.

It is straightforward to demonstrate that the time dependent portions of the four viscous terms in Eq. 5 are only proportional if

$$\delta_1 \propto \delta \propto \delta_3 \propto (t - t_o)^{1/2}. \quad (6)$$

This implies that all three length scales must have the same virtual origin.

Further, the time-dependent portions of the convective and the unsteady terms in Eq. 5 are only proportional to the time-dependent portions of these viscous terms if

$$\left[ \frac{Q^{i,j}}{\delta} \frac{d\delta}{dt} \right] \propto \left[ \frac{U_s Q^{i,j}}{\delta} \right] \Rightarrow \left[ \frac{1}{\delta} \frac{d\delta}{dt} \right] \propto \left[ \frac{U_s}{\delta} \right] \quad (7a)$$

and

$$\left[ \frac{U_s Q^{i,j}}{\delta} \right] \propto \left[ \frac{\nu Q^{i,j}}{\delta^2} \right] \Rightarrow \left[ \frac{U_s}{\delta} \right] \propto \left[ \frac{\nu}{\delta^2} \right]. \quad (7b)$$

These constraints are satisfied if the three time scales  $\delta/U_s$  (a characteristic time scale of the mean strain rate),  $\delta^2/\nu$  (a viscous time scale), and  $(1/\delta \, d\delta/dt)^{-1}$  (a characteristic time scale of the spreading of the flow) are proportional. Thus, the ratio of these time scales are constant; *i.e.*,

$$\beta = \frac{1}{U_s} \frac{d\delta}{dt} \propto \text{const} \quad (8a)$$

and

$$Re_\delta = \frac{U_s \delta}{\nu} \propto \text{const}, \quad (8b)$$

which are the constraints derived in the analysis of the single-point equations.

The constraint that the Reynolds number is a constant is a gratifying result since a single length scale was used to define each of the similarity coordinates in Eq. 3f. Thus, it was implicitly assumed that all of the physically relevant length scales in the flow grow in proportion as the flow evolves; an assumption that is generally thought to be valid in a constant-Reynolds-number flow (Batchelor 1953). The functional form of the solutions will, of course, depend on the ratios of the physically relevant length scales (or the Reynolds number).

The constant  $\beta$  that appears in the equations is analogous to the constant that George (1989) found in the governing equation for the turbulent kinetic energy in the spatially evolving wake. It is very likely that the value of this ratio depends on the coherent structures in the flow, and it is through this constant that their influence is incorporated into the equations for the similarity solutions.

The time-dependent portions of the rest of the terms in Eq. 5 are proportional if

$$P_1^i \propto U_s Q^{i,k}, P_1^j \propto U_s Q^{k,j}, \quad (9a)$$

and

$$T_1^{k,i,j} \propto T_2^{i,k,j} \propto U_s Q^{i,j}. \quad (9b)$$

These expressions must be satisfied for any choice of  $k$ . The choice for  $Q^{i,j}$  is not uniquely determined from Eq. 5; however,  $Q^{i,j}$  is not arbitrary since the similarity solution for the two-point velocity correlation tensor must be consistent with the similarity solution derived for the single-point moments (Moser *et al.* 1995). Thus, it follows that

$$Q^{i,j} \propto U_s^2. \quad (10)$$

Of course, these constants of proportionality may be functions of  $\beta$  or  $Re_\delta$ .

Thus, the governing equations for the two-point velocity correlation tensor in the temporally evolving wake admit similarity solutions, of which the similarity solution for the single-point Reynolds stresses are a special case. It is straightforward to demonstrate that the governing equations for the similarity solutions include the constants  $Re_\delta$  and  $\beta$ . Thus, in general, the similarity solutions are functions of these two ratios whose values depend on the source conditions of the flow. In many flows, the initial conditions are not consistent with the hypothesized similarity solution so these solutions are, at most, an approximation of the asymptotic state of the flow (as with the single-point similarity solutions).

### 2.2 Implications of the similarity hypothesis

When a similarity solution exists for the two-point velocity tensor, other statistical measures that can be determined directly from this two-point correlation also have similarity solutions. In many cases, these results provide useful predictions to compare with data in order to test the similarity hypothesis.

For example, when a similarity solution exists for the two-point velocity correlation tensor, the one-dimensional spectra in the  $x_1$ -direction given by

$$F_{ij}^1(k_1, x_2, x'_2, \gamma) = \frac{1}{2\pi} \int_{-\infty}^{\infty} R_{i,j}(\zeta, x_2, x'_2, \gamma) e^{-ik_1\zeta} d\zeta$$

(where  $R_{i,j} = \overline{u_i u'_j}$ ) can be written as

$$F_{ij}^1(k_1, x_2, x'_2, \gamma) = [Q_{i,j}\delta] \tilde{F}_{ij}^1(\tilde{k}_1, \eta, \eta', \zeta), \quad (11a)$$

where the similarity solution for the one-dimensional spectra is given by

$$\tilde{F}_{ij}^1(\tilde{k}_1, \eta, \eta', \zeta) = \frac{1}{2\pi} \int_{-\infty}^{\infty} q_{i,j}(\xi, \eta, \eta', \zeta) e^{-i\tilde{k}_1\xi} d\xi \quad (11c)$$

and  $\tilde{k}_1$  is the given by

$$\tilde{k}_1 = k_1\delta. \quad (11b)$$

A similar relationship can be derived for the one-dimensional spectra in the  $x_3$ -direction. Thus, when a similarity solution exists for the two-point velocity correlation tensor, the one-dimensional spectra of the field maintain the same shape while continuously shifting downward and to lower wavenumbers as the flow spreads.

It is also straightforward to demonstrate that many of the classically defined turbulent length scales are proportional to the similarity length scale. For example, the Taylor microscales given by

$$\lambda_{\alpha,\beta}^k = \left\{ -2\overline{u_\alpha u_\beta} \left( \frac{\partial^2 R_{\alpha,\beta}}{\partial \tilde{x}_k^2} \Big|_{\tilde{x}_k = x_k - x'_k = 0} \right)^{-1} \right\}^{1/2} \quad (12)$$

can be written as (Ewing 1995)

$$\lambda_{\alpha,\beta}^k = [\delta] \tilde{\lambda}_{\alpha,\beta}^k(\eta, Re_\delta, \beta), \quad (13)$$

It is also straightforward to show that the integral length scales and the Kolmogorov length scale are proportion to the similarity length scale (Ewing 1995).

A number of other interesting implications of the two-point similarity hypothesis, such as similarity solutions for the moments related to the two-point velocity-gradient correlation tensor (*e.g.*, the two-point vorticity correlation or the dissipation of the turbulent kinetic energy in the flow), are discussed in Ewing (1995) and Ewing *et al.* (1995).

### 2.3 Comparison with simulation data

Although the previous analysis demonstrated that the hypothesized similarity solutions are consistent with the equations of motion, this does not ensure that these solutions are an accurate description of real flows. In this case the predictions of the similarity hypothesis for the two-point velocity correlation tensor are compared to the data from two Direct Numerical Simulations of the temporally evolving wake computed by Moser and Rogers (1994). These simulations were carried out in finite boxes with periodic boundary conditions in the homogeneous directions in contrast to the theory, which was developed for a wake in an infinite domain. Consequently, the theory cannot exactly approximate the flow in these simulations. However, it is generally argued that the evolution of the scales of motion that are ‘much’ smaller than the dimension of the boxes in the periodic directions should be similar to the evolution of those in an infinite wake. Thus, a comparison between the predictions of the similarity hypothesis and the data from the simulations is essentially a test of both the similarity hypothesis and this idea. Agreement between the predictions of the theory and the data lends support to both. (Experimentalists experience the very same problem when data from finite experimental rigs, such as wind tunnels, are used to test hypotheses developed for infinite flow; *e.g.*, George and Gibson 1992).

The initial conditions for the wake simulations were generated using two realizations from a turbulent boundary layer simulation yielding a wake with a Reynolds number, given by

$$Re_{\delta_d} = \frac{\int_{-\infty}^{\infty} (U_1 - U_{1\infty}) dx_2}{\nu}, \quad (14)$$

of 2000. In the first (unforced) wake simulation the base initial conditions were used to initiate the flow while in the second (forced) wake simulation the  $u_1$  and  $u_2$  velocity components of the spanwise two-dimensional modes were amplified by a factor of 5. These simulations are computed in periodic boxes of length  $50\delta_d$  in the  $x_1$ -direction and  $12.5\delta_d$  in the  $x_3$ -direction, where  $\delta_d$  is the initial displacement thickness of the wake. Moser and Rogers (1994) found that the data from both simulations were approximately in agreement with the predictions of the similarity hypothesis for a period of the flow’s evolution. For example, it is evident from Figs. 2a and 2b that the Reynolds number of both flows is approximately constant

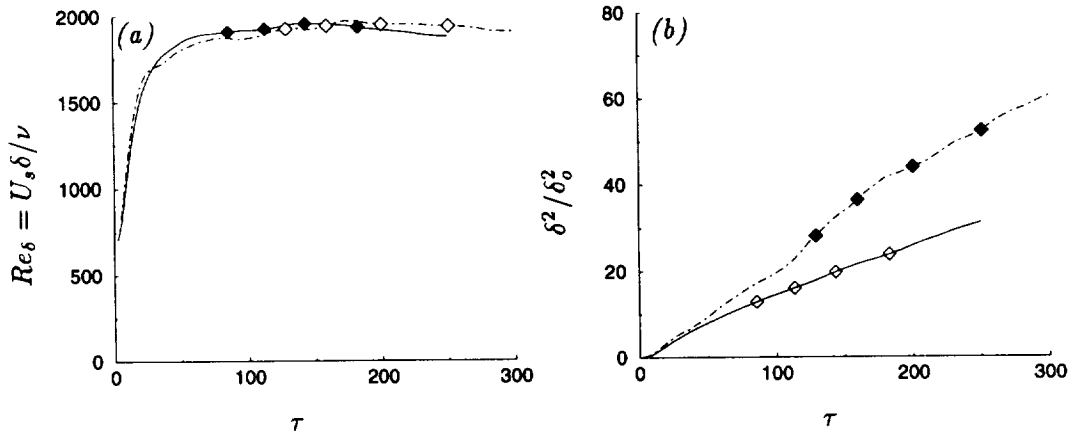


FIGURE 2. Evolution of the Reynolds number and similarity length scale: — : unforced wake simulation; ---- : forced wake simulation;  $\diamond$  : location of points used to examine the two-point similarity hypothesis.

and the square of the similarity length scales in the flows grow approximately linearly, as predicted in the similarity analysis, for a significant time period. The two-point similarity hypothesis is tested using data from four points in this range, indicated by the diamonds in Figs. 2a and 2b.

The unscaled one-dimensional spectra  $F_{11}^1$  and  $F_{22}^1$  at the centerline of the two wakes (spatially averaged in the  $x_3$ -direction) are illustrated in Figs. 3a and 3b. The spectra exhibit peaks in the low-wavenumber region that are inconsistent with the similarity hypothesis since they occur at the same wavenumber in physical variables. However, it is not anticipated that the similarity hypothesis should collapse the spectra in this region because it is likely that these motions are affected by the periodic boundary conditions or, conversely, the coarse discretization of wave space at these scales. In contrast, the spectra in the high-wavenumber region shift downward and to the left as the flow evolves, in agreement with the predictions of the similarity hypothesis. The amplitude of the spectra in this high-wavenumber region differ by a factor of approximately 3–4 so they should provide a good test of the similarity hypothesis.

The scaled one-dimensional spectra  $\tilde{F}_{11}^1$  at the centerline and the half-deficit point,  $\eta = 0.5$ , in the unforced wake are illustrated in Fig. 4, while the scaled one-dimensional spectra  $\tilde{F}_{22}^1$  at the same points in the forced wake simulation are illustrated in Fig. 5. In both of these figures the data from the half-deficit point in the wake are shifted up by a order of magnitude. Overall there is excellent collapse of the data for the region where  $\tilde{k}_1 \geq 15\Delta\tilde{k}_1$ , indicating that the statistical measures of all but the largest motions evolve as predicted by the similarity hypothesis. There is some discrepancy between the predictions and the data at the largest wavenumbers; however, these variations occur because the effective resolution of the simulations varies as the flow evolves (Ewing 1995). The one-dimensional spectra of the correlations in the  $x_3$ -direction (Ewing 1995) exhibit better collapse than the



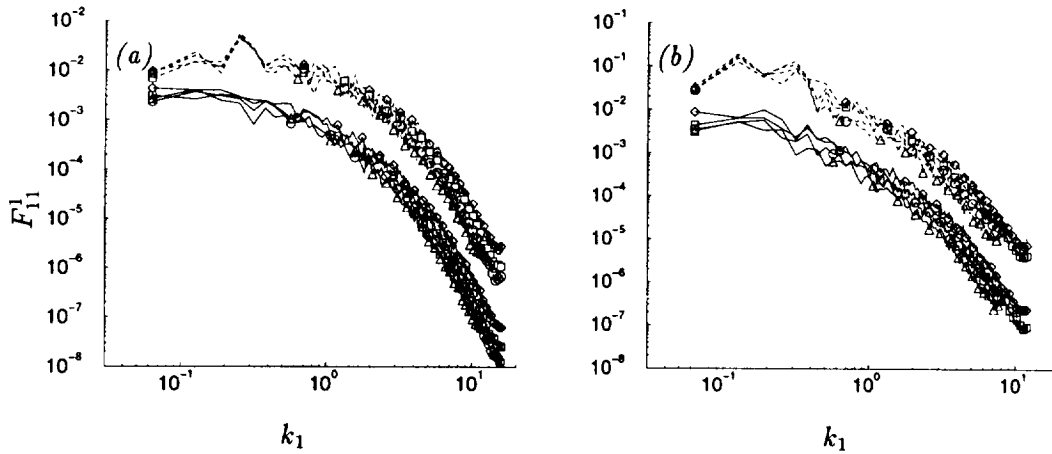


FIGURE 3. Unscaled one-dimensional spectra in (a) the unforced wake, (b) the forced wake: — :  $F_{11}^1$ , ---- :  $F_{22}^1$ . In (a)  $\delta/\delta_d$  is equal to: 3.494  $\diamond$ , 4.008  $\square$ , 4.446  $\circ$ , and 4.884  $\triangle$ . In (b)  $\delta/\delta_d$  is equal to: 5.306  $\diamond$ , 6.037  $\square$ , 6.636  $\circ$ , and 7.235  $\triangle$ .

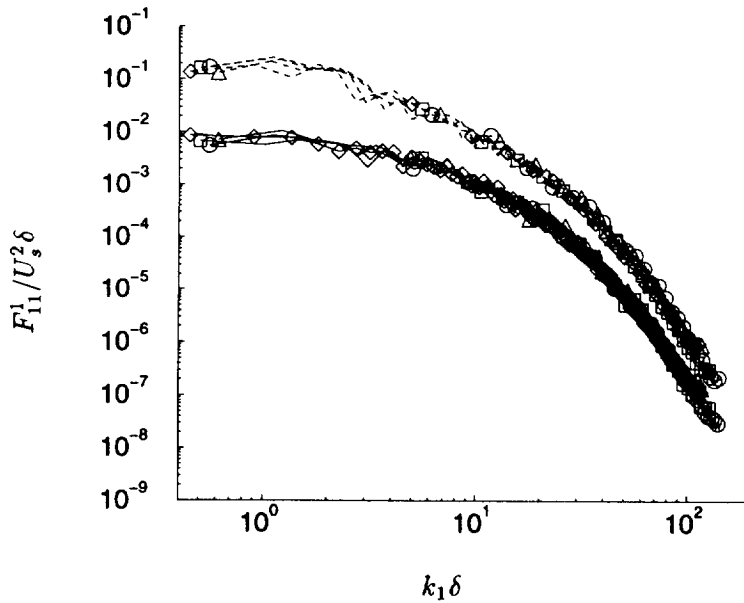


FIGURE 4. Scaled one-dimensional spectra,  $\tilde{F}_{11}^1$  in the unforced wake at —  $\eta = 0.0$  and ----  $\eta = 0.5$ .  $\delta/\delta_d$  is equal to; 3.494  $\diamond$ , 4.008  $\square$ , 4.446  $\circ$ , and 4.884  $\triangle$ .

spectra in the  $x_1$ -direction (partially because these spectra are spatially averaged in the  $x_1$ -direction, which is 4 times longer than the  $x_3$ -direction used to average  $\tilde{F}_{\alpha\alpha}^1$ ).

The large-scale motions make a contribution to the two-point velocity correlation tensor for all separation distances. Consequently, the structure functions in the

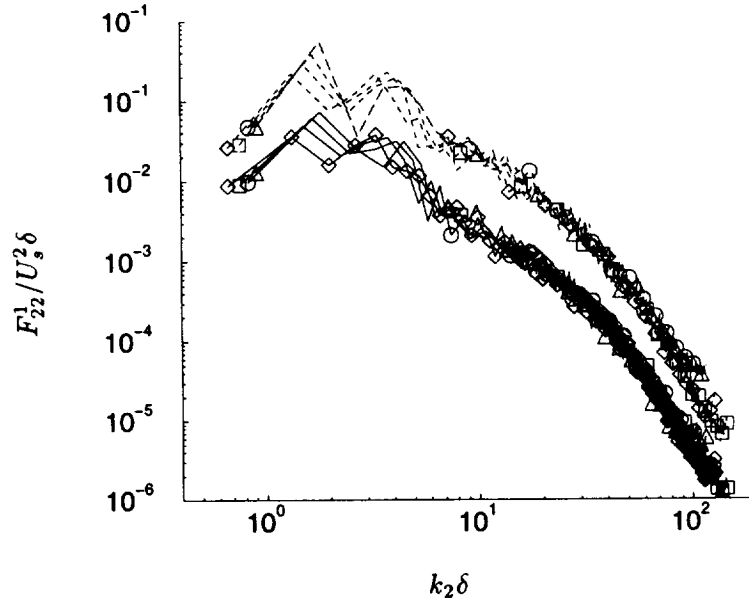


FIGURE 5. Scaled one-dimensional spectra,  $\tilde{F}_{22}^1$  in the forced wake at —  $\eta = 0.0$  and ----  $\eta = 0.5$ .  $\delta/\delta_d$  is equal to; 5.306  $\diamond$ , 6.037  $\square$ , 6.636  $\circ$ , and 7.235  $\triangle$ .

$x_2$ -direction, given by

$$\overline{(u_\alpha - u'_\alpha)^2} = \overline{u_\alpha^2} + \overline{u'^2_\alpha} - 2R_{\alpha,\alpha}(x_2, x'_2) \quad (15)$$

are used to compare the prediction of the similarity hypothesis and the data, since they are more measures of the motions whose sizes are on the order of the separation distance between the points. The structure functions for  $\alpha = 1$  centered around the centerline and the half-deficit point in the unforced wake, scaled with appropriate similarity variables, are shown in Figs. 6a and 6b. In both cases the profiles from the four different times collapse for small and intermediate separation distances, suggesting again that the statistical measures of all but the largest scales of motion in the flow are evolving as predicted by the similarity hypothesis. The structure functions from the forced wake simulation also collapse for small and intermediate separation distances when they are scaled using similarity variables (Ewing 1995).

#### 2.4 Scalar fields

The similarity analysis was also extended to the governing equations for a passive scalar field. It was demonstrated that these equations admit similarity solutions for both a scalar field with a mean deficit in the wake region and a scalar field where the mean value in the two free streams differ. The predictions of the similarity hypothesis were compared to data from the simulations, which were computed with this second type of scalar field. However, the variations of the two-point scalar correlation in the simulations were much smaller than the variations of the two-point velocity correlation tensor (as predicted by the similarity hypothesis). As

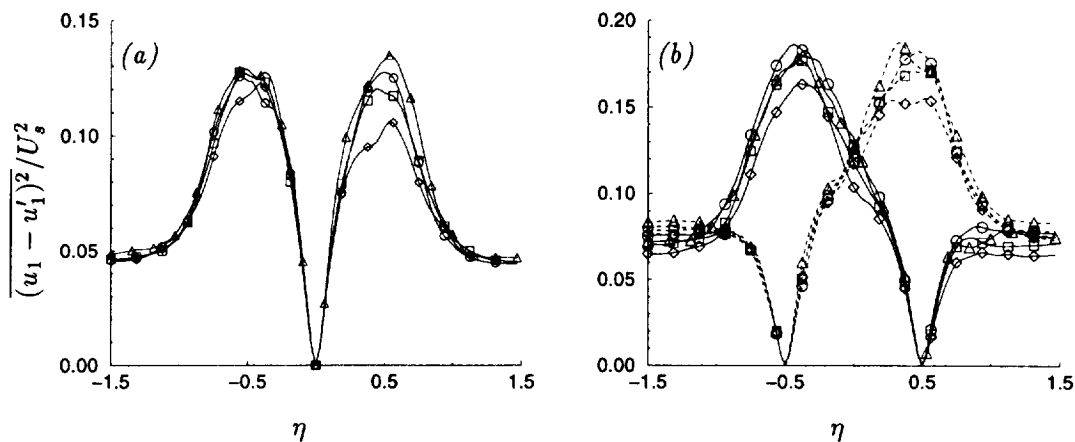


FIGURE 6. Scaled structure functions about (a)  $\eta = 0$  (b)  $\eta = 0.5$ .  $\delta/\delta_d$  is equal to: 3.494  $\diamond$ , 4.008  $\square$ , 4.446  $\circ$ , and 4.884  $\triangle$ .

a result, the data from the period where the simulations were approximately self-similar did not vary sufficiently to rigorously test the predictions of the similarity hypothesis for the scalar field. Further details of this comparison can be found in Ewing (1995).

### 3. Conclusions

The analysis demonstrated that the governing equations for the two-point velocity correlation tensor in the temporally evolving wake admit similarity solutions, which include the similarity solutions for the single-point moment as a special case. The resulting equations for the similarity solutions include two constants,  $\beta$  and  $Re_\delta$ , that are ratios of three characteristic time scales of processes in the flow: a viscous time scale, a time scale characteristic of the spread rate of the flow, and a characteristic time scale of the mean strain rate. The values of these ratios depend on the initial conditions of the flow and are most likely measures of the coherent structures in the initial conditions. The occurrences of these constants in the governing equations for the similarity solutions indicates that these solutions, in general, will only be the same for two flows if these two constants are equal (and hence the coherent structures in the flows are related).

The comparisons between the predictions of the similarity hypothesis and the data presented here and elsewhere (Ewing 1995) indicate that the similarity solutions for the two-point correlation tensors provide a good approximation of the measures of those motions that are not significantly affected by the boundary conditions caused by the finite extent of real flows. Thus, the two-point similarity hypothesis provides a useful tool for both numerical and physical experimentalist that can be used to examine how the finite extent of real flows affect the evolution of the different scales of motion in the flow. The similarity analysis of the governing equations for the multi-point correlations can be extended to a wide range of spatially and temporally evolving flows using the methodology outlined by Ewing (1995), so this technique

can be used to examine the effect of finite boundaries on the evolution of a number of different flows.

## REFERENCES

- EWING, D. & GEORGE, W. K. 1994 Applications of a similarity hypothesis to the proper orthogonal decomposition for spatially evolving flows. In *Proc. of the Int. Symp. on Turb. Heat and Mass Trans.*, Lisbon, Portugal.
- EWING, D. 1995 On multi-point similarity solutions in turbulent free-shear flows. *Ph.D. Dissertation*, State University of New York at Buffalo.
- EWING, D., GEORGE, W. K., ROGERS, M. M. & MOSER, R. D. A similarity hypothesis for the two-point correlations in a temporally evolving, plane wake *J. Fluid Mech. in preparation*.
- GEORGE, W. K. 1989 The self-similarity of turbulent flows and its relation to initial conditions and coherent structures. In *Advances in Turbulence*. edit. W. K. George and R. E. Arndt, Hemisphere Publishing.
- GEORGE, W. K. & GIBSON, M. M. 1992 The self-preservation of homogeneous turbulence. *Expt. in Fluids*. **13**, 229.
- GEORGE, W. K. 1994 Some new idea for similarity of turbulent shear flows. In *Proc. of the Int. Symp. on Turb. Heat and Mass Trans.*, Lisbon, Portugal.
- GRANT, H. L. 1958 The large eddies of turbulent motion. *J. Fluid Mech.* **3**, 149.
- MOSER, R. D. & ROGERS M. M. 1994 Direct simulation of a self-similar plane wake. NASA Tech. Memo, TM 108815.
- MOSER, R. D., ROGERS, M. M., & EWING, D. 1995 *J. Fluid Mech. in preparation*.
- PAYNE, F. R. & LUMLEY, J. L. 1967 Large eddy structure of the turbulent wake behind a circular cylinder. *Phys. Fluids Supp.* **10**, 194.
- TENNEKES, H. & LUMLEY, J. L. 1972 *A First Course in Turbulence*. MIT Press.
- WYGNANSKI, I., CHAMPAGNE, F., & MARASLI, B. 1986 On the large-scale structures in two-dimensional, small-deficit, turbulent wakes. *J. Fluid Mech.* **168**, 31.